^{13}C-NMR relaxation study of heparin–disaccharide interactions with tripeptides GRG and GKG

Dmitri MIKHAILOV*, Kevin H. MAYO*†, Azra PERVIN‡ and Robert J. LINHARDT‡

*Departments of Biochemistry and Lab Medicine & Pathology, Biomedical Engineering Center, University of Minnesota Medical School, 420 Delaware Street, S. E., Minneapolis, MN 55455, U.S.A., and ‡Department of Medicinal and Natural Products Chemistry, College of Pharmacy, The University of Iowa, 115 S. Grand Ave., Iowa City, Iowa 52242, U.S.A.

Heparin is a polydisperse sulphated copolymer consisting mostly of $1 \rightarrow 4$ linked glucosamine and uronic acid residues, i.e. 2-deoxy-2-sulphamido-D-glucopyranose 6-sulphate and L-idopyranosyluronic acid 2-sulphate. ^{13}C NMR has been used to study the interactions of heparinase-derived and purified heparin disaccharide with N- and C-terminally-blocked tripeptides GRG and GKG. Titration of the disaccharide with peptide indicates that GRG binds the disaccharide more strongly than does GKG, with interactions in either case being stronger at uronate ring positions. In the presence of GRG, a carboxylate pK_a depression suggests electrostatic interactions between the arginine guanidinium group and the uronate carboxylate group. ^{13}C relaxation data have been acquired for all disaccharide and peptide carbons in the presence and absence of GRG and GKG. ^{13}C relaxation rates for the disaccharide are significantly faster in the presence of peptide, especially with GRG. Analysis of these relaxation data has been done in terms of molecular diffusion constants, $D_\perp$ and $D_\parallel$, and an angle α between $D_\parallel$ and a molecular frame defined by the moment of inertia tensor calculated for an internally rigid disaccharide. Disaccharide conformational space in these calculations has been sampled for both uronate half-chair forms ($^2H_1$ and $^1H_2$) and over a range of glycosidic bond angles defined by motional order parameters and inter-residue nuclear Overhauser effects ($\pm 30°$ from the average). In the absence of peptide, the ratio $D_\perp/D_\parallel$ falls between 0.4 and 0.7; therefore molecular diffusion occurs preferentially about $D_\parallel$, which runs through both disaccharide rings. In the presence of peptide, $D_\perp/D_\parallel$ is decreased, indicating that GRG is oriented along $D_\parallel$ and proximal to the uronic acid ring. A model for this is shown.

INTRODUCTION

Heparin is mainly a polydisperse sulphated copolymer of $1 \rightarrow 4$ linked glucosamine and uronic acid residues. Most of the heparin molecule is accounted for by this repeating disaccharide unit that consists of L-idopyranosyluronic acid (IdoA) 2-sulphate and 2-deoxy-2-sulphamido-D-glucopyranose ($GlcNSO_3$) 6-sulphate [1,2]. This repeating sequence represents at least 85% of heparins from beef lung and about 75% of those from intestinal mucosa [3]. The balance of the molecule is constituted largely of residues of 2-acetamido-2-deoxy-D-glucopyranose and D-glucopyranosyluronic acid, although their modes of bonding and distribution within the polymer, as well as their degrees of sulphation, have yet to be established unequivocally.

The accumulated information about GAG–protein interactions raises intriguing questions concerning specificity. Do GAG-binding polypeptides display any 'consensus' structure? How do we define specificity in the context of a polydisperse polysaccharide? Is 'uniqueness' on the part of GAG sequence involved in binding a prerequisite for such specificity? An understanding of how heparin functions at the molecular level requires thorough information about the structure and conformation of the polymer chain and how it interacts with specific peptide residues. The ability of many proteins to bind heparin and related polysulphated glycosaminoglycans (GAGs), might reflect functional relationships *in vivo* and is often exploited in purification protocols. Protein ligands for GAGs include enzymes (e.g. lipoprotein lipase), enzyme inhibitors (e.g. antithrombin-III), extracellular matrix proteins (e.g. fibronectin), certain growth factors [e.g. fibroblast growth factors (FGFs)], viral coat glycoproteins and several others (reviewed in [4–6]). FGF-2, for example, binds avidly to a heparin hexasaccharide sequence composed of three consecutive -IdoA(2-OSO_3)-$GlcNSO_3$(6-OSO_3)-disaccharide units (i.e. the predominant 'building block' in heparin) [7,8]. The number of proteins with GAG-binding properties implicated in their cell-biological roles is steadily increasing. The list includes chemokines [9–11], other types of growth factors (vascular endothelial growth factor [12], hepatocyte growth factor [13], heparin-binding epidermal growth factor-like growth factor [14,15]), L-selectin [16], the platelet/endothelial cell adhesion molecule-1 [17] and the neuronal heparin-binding growth-associated molecule [18].

Considerable effort has gone into identifying protein domains that specifically interact with heparin/heparan sulphate sequences and into pinpointing consensus sequences at the peptide level. Information gained along these lines has been interpreted in terms of relatively short heparin-binding 'consensus sequences' involving clusters of basic amino acids [17,19–22]. There is now compelling evidence from crystal structures of different heparin-binding proteins, such as (cleaved) antithrombin [23], lipoprotein lipase [24] and basic fibroblast growth factor [FGF-2] [25], that the key amino acids comprising heparin-binding domains may actually be located in different peptide sequences that are spatially proximal. As a result of the tertiary structure of the protein, such sequences might converge to form a composite GAG-binding site that would accommodate relatively small oligosaccharide ligands (e.g. the antithrombin-binding pentasaccharide sequence in heparin [23]). Two amino acid residues, lysine and arginine, stand out as being essential for heparin binding (see, for example, [26]). Questions about pref-

Abbreviations used: COSY, two-dimensional NMR correlated spectroscopy; FGF, fibroblast growth factor; GAG, glycosaminoglycan; $GlcNSO_3$, 2-deoxy-2-sulphamido-D-glucopyranose; IdoA, L-idopyranosyluronic acid, NOE, nuclear Overhauser effect.

† To whom correspondence should be addressed.

erential interactions between lysine and arginine side chains and various chemical groups on heparin (or GAGs in general) are difficult to address by the relatively high charge density on GAGs in particular. It is primarily for this reason that a reductionist approach is taken in the present study, where ^{13}C-NMR relaxation has been used to study interactions of heparinase-digested and homogeneously purified heparin disaccharide, with N- and C-terminally blocked tripeptides GRG and GKG. Studying simple arginine- and lysine-containing tripeptides and small, homogeneous heparin disaccharide might provide key insight into the nature of the interactions of larger protein–heparin molecules.

MATERIALS AND METHODS

Heparin disaccharide isolation

Approx. 20 mg of heparin was dissolved in 10 ml of distilled water and dialysed exhaustively, freeze-dried, and prepared at exactly 20.0 mg/ml in distilled water [27]. To 50 μl of heparin (20 mg/ml) was added 450 μl of sodium phosphate buffer (5 mM sodium phosphate, pH 7, and 200 mM sodium chloride) containing 15 μ-units heparinase. The reaction mixture was incubated at 30 °C for 8 h. At reaction completion, the depolymerization mixture was separated and individual low-molecular-mass heparin fractions were isolated by HPLC as discussed previously [28].

Peptide synthesis

GRG and GKG were synthesized on a Milligen Biosearch 9600 automated peptide synthesizer using Fmoc–BOP chemistry [29]. To avoid electrostatic contributions from N- and C-termini, the C-terminal carboxylate group was amidated and the N-terminal amine was acetylated. After the sequence had been obtained, the peptide support and side-chain protection groups were acid cleaved (with trifluoroacetic acid and scavenger mixture). Crude peptides were analysed for purity on a Hewlett-Packard 1090M analytical HPLC with a reverse-phase C18 VyDac column. Peptides were generally about 90 % pure. Further purification was done on a preparative reverse-phase HPLC C18 column with an elution gradient of 0–60 % (v/v) acetonitrile with 0.1 % trifluoroacetic acid in water. Peptides then were analysed for amino acid composition on a Beckman 6300 amino acid analyser by total hydrolysis (6 M HCl at 110 °C for 18–20 h) and by mass spectrometry. Final peptide purity was greater than 95 %.

NMR measurements

For NMR measurements, freeze-dried heparin disaccharide and tripeptides were dissolved in ^2H_2O. Peptide and sugar concentrations were in the range 0.5–150 mM. pH was adjusted to the desired value by adding microlitre quantities of NaO^{2}H or ^{2}HCl to the sample. For most experiments, the temperature was controlled at 5 °C to achieve shorter relaxation rates and a greater population of peptide-bound disaccharide. All NMR spectra were acquired on Bruker AMX-600 and AM-250 NMR spectrometers operating at ^{13}C frequencies of 150 and 62.5 MHz respectively. Heparin disaccharide ring ^{13}C resonance assignments were taken from Merchant et al. [30].

Proton–proton coupling constants were derived from a high-resolution double quantum filtered two-dimensional NMR correlated spectroscopy (COSY) experiment [31,32] acquired in the phase-sensitive mode by using time proportional phase incrementation [33,34]. The residual water resonance was suppressed by direct irradiation (0.6 s) at the water frequency during the relaxation delay between scans. Spectra were collected as 1024 t_1 experiments each with 4096 complex data points over a spectral width of 5 kHz in both dimensions, with the carrier placed on the water resonance. A total of 32 scans were time-averaged per t_1 experiment. The data were processed directly on the Bruker AMX-600 X-32 or offline on a Bruker Aspect-1 workstation with the Bruker UXNMR data processing program. Data sets were multiplied in both dimensions by 0–60°-shifted sine-bell or Lorentzian to Gaussian transformation functions and generally zero-filled to 2048 in the t_1 dimension before Fourier transformation.

Spin–lattice relaxation was monitored by the inversion-recovery method with and without broad-band proton decoupling. The number of acquisitions was varied from 5000 to 16000 to maintain a signal-to-noise ratio greater than 6. At least ten partly relaxed spectra were acquired for each relaxation experiment. To reduce errors from radiofrequency field inhomogeneities, the composite 180° pulse ($90°_x - 180°_y - 90°_x$) was used. T_1 values were calculated from the initial slope of relaxation rate curves by using the method described by Daragan and Mayo [35]. To minimize the error in determining these rates, a least-squares method with weighted functions, e.g. $A(t) = \exp(-2W_W t)$, was used [35]. W_W was calculated by minimizing the function $\Sigma_i[I_0 - I_i - A\exp(-W_W t_i)]^2$, where I_0 and I_i are equilibrium and transient values respectively of resonance intensities. To calculate the relaxation rate, W, minimization of the function:

$$S = \Sigma_i \exp(-2W_W t_i)[I_0 - I_i - A\exp(-Wt_i)]^2 \quad (1)$$

was performed. This method reduces errors arising from inaccuracies normally present at the tail of relaxation curves plotted on the semilogarithmic scale. Statistical errors in determining spin–lattice relaxation rates were less than about 5 %.

Motional order parameters, S^2, (model free approach; [36,37]) were calculated for the heparin disaccharide by using ^{13}C methyne T_1 values at two ^{13}C-NMR frequencies, 62.5 and 150 MHz. Values of τ_1 were initially fixed at 10^{-11} s, whereas τ_0 and S^2 were allowed to vary. τ_0 and S^2 were found to be relatively insensitive to changes in τ_1. Because disaccharide A and B rings are of nearly equal mass, motional recoil effects [38] can greatly influence relaxation-derived order parameters. These recoil effects were taken into account as described by Daragan and Mayo [38].

Diffusion tensor calculations

For the model of anisotropic rotational diffusion of a symmetric ellipsoid, rotations can be characterized by two rotational diffusion coefficients: $D_\parallel$, describing rotations about the molecular symmetry axis, and $D_\perp$, describing rotations orthogonal to this axis. For the heparin-derived disaccharide molecule, moment of inertia tensor calculations show that $I_x \approx I_y \approx 2I_z$ such that $D_\parallel > D_\perp$, and the symmetry axis is the main molecular rotation axis. Autocorrelation times can be written as [39]:

$$\tau_{CH} = a^{CH}{}_0/D_0 + a^{CH}{}_1/D_1 + a^{CH}{}_2/D_2$$

where

$$a^{CH}{}_0 = P_2(\cos\theta_{CH})P_2(\cos\theta_{CH})$$

$$a^{CH}{}_1 = 3\cos^2\theta_{CH}\sin^2\theta_{CH}$$

$$a^{CH}{}_2 = (3/4)\sin^4\theta_{CH}$$

$P_2(x) = 0.5\ (3x^2 - 1)$ is the second-order Legendre polynomial. θ_{CH} are the polar angles of the CH vectors in the co-ordinate system X_D, Y_D, Z_D, where the Z_D axis is directed along the main rotation axis. The coefficients D_μ, $\mu = 0, 1, 2$, can be written as:

$$D_\mu = 6D + (D_\parallel - D_\perp)\mu^2$$

In terms of molecular diffusion, the parameters $D_{\parallel}$ and $D_{\perp}$ can be determined from the experimental values of T_1 relaxation times obtained for two ^{13}C frequencies that represent five non-redundant motional vectors.

For the initial moment of inertia and diffusion tensor calculations, the disaccharide structure was based on a heparin dodecamer conformation [40] (Brookhaven structural database) from which was excised a disaccharide unit with correct stereochemistry. A double bond was introduced into the uronic acid A ring between the A4 and A5 carbon atoms, and the internal energy of the disaccharide was then minimized by using the electrostatic force field with a distance-dependent dielectric constant (4*r*) (Biosym, Inc.) to approximate solvent effects. Moreover, because the uronic acid residue can exist in solution as two ring conformers, $^2H_1$ and $^1H_2$ (10 % and 90 % respectively, according to Ragazzi et al. [41]), calculations were performed with both forms. With an electrostatic force field, the resulting heparin disaccharide structure has the uronate and glucosamine rings in normally observed conformations (major $^1H_2$ form of uronate with the ring oxygen and C-3, C-4 and C-5 carbons in the same plane and the glucosamine ring in the chair form) with the uronate H-1 and glucosamine H-4 protons in close proximity. This is consistent with nuclear Overhauser effect (NOE) results discussed later.

Optimization of the two half-chair conformers of uronate resulted in the $^2H_1$ and $^1H_2$ forms with an energy difference of 3.5 kcal/mol. Although this energy difference is considerably larger than the 1.0 kcal/mol difference reported by Ragazzi et al. [41], the $^1H_2$ form is the predominant form *in vacuo* from either calculation. Ragazzi et al. [41] concede that their minimum-energy structure gives 'rather unusual values for the torsion angles at the glycosidic linkage.' The difference in conformer energies is the result of using weaker electrostatic potentials in electrostatic force field compared with the MM2/87 force field used by Ragazzi et al. [41] and is accounted for mostly by differences in the glycosidic bond angles. The Ragazzi et al. [41] $^1H_2$ conformer, however, does agree with our ^1H–^1H NOE data discussed in the Results section. Because moment of inertia and diffusion tensor calculations are sensitive to the inter-ring disaccharide conformation, which is fixed during the calculation, a range of disaccharide $1 \rightarrow 4$ bond angle orientations was used to sample the distribution of experimentally allowed conformations. This is discussed further in the Results section. All calculations were performed on a Silicon Graphics Challenge-L computer (four R4400 CPUs).

RESULTS

Figure 1 shows the chemical bond structure of the heparin disaccharide investigated in this study. The uronate and glucosamine rings are identified with the letters A and B respectively. Therefore the carbons discussed below will be identified as A1, A2, A3, A4, B1, B2, B3, B4, B5 and B6. A5 and A6 carbons have not been investigated owing to their long relaxation times, absence of bonded protons and the number of transients needed for good signal-to-noise ratios.

pH titration data with the heparin disaccharide are shown in Figure 2 (△). Because the C-4 of the uronic acid ring is shifted the most, owing to its proximity to the carboxylate group, only its chemical shift against the solution pH has been plotted in Figure 2. By using the Henderson–Hasselbalch equation, a carboxylate pK_a of 3.15 ± 0.01 is derived from a fit of these data (solid line). This value is nearly the same as that found by Wang et al. [42]. Within the pH range studied, the sulphates do not change their ionization state as judged by minimal chemical shift changes in other carbon resonances. Heparin sulphate and carboxylate group pK_a values are 0.5–1.5 [43] and 2.8–3.1 [42] respectively. Above pH 4.5, therefore, all acidic groups are

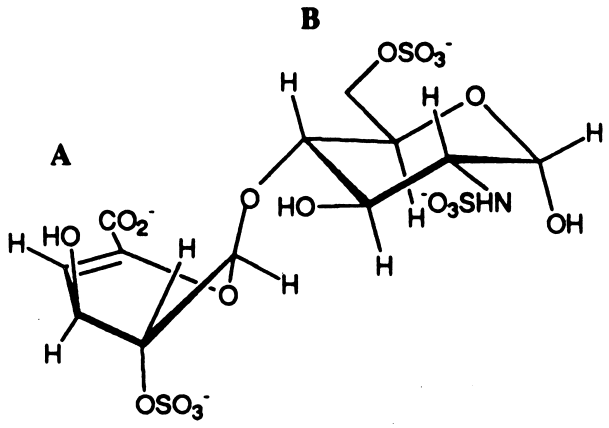

Figure 1 Heparin disaccharide chemical structure

The A and B rings for the heparin disaccharide molecule used in these studies are shown in the half chair and chair conformations respectively. The orientation of one ring with respect to the other is not correct and is given in this way only to show the individual ring conformations clearly. In solution, NOEs show that A1-H is proximal to B4-H and the B ring is rotated about 180° with respect to the A ring as depicted here.

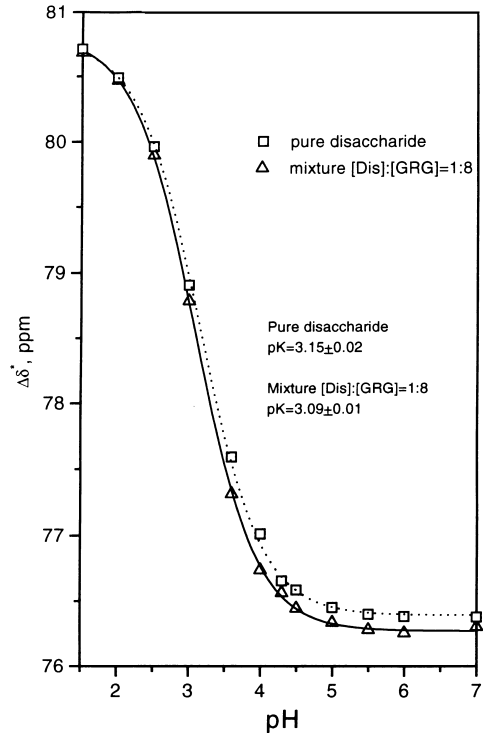

Figure 2 ^{13}C chemical shift change in heparin disaccharide with pH

Heparin disaccharide in the presence (△) and absence (□) of an 8-fold molar excess of GRG is plotted against the solution pH. The pH was adjusted by adding microlitre quantities of ^2HCl or NaO^2H to a 0.5 ml ^2H_2O sample volume at 278 K. No corrections were made for isotope effects. Curve fitting was done by using the Henderson–Hasselbalch equation. Dotted and solid lines represent curves for chemical shift data in the absence and presence of peptide respectively.

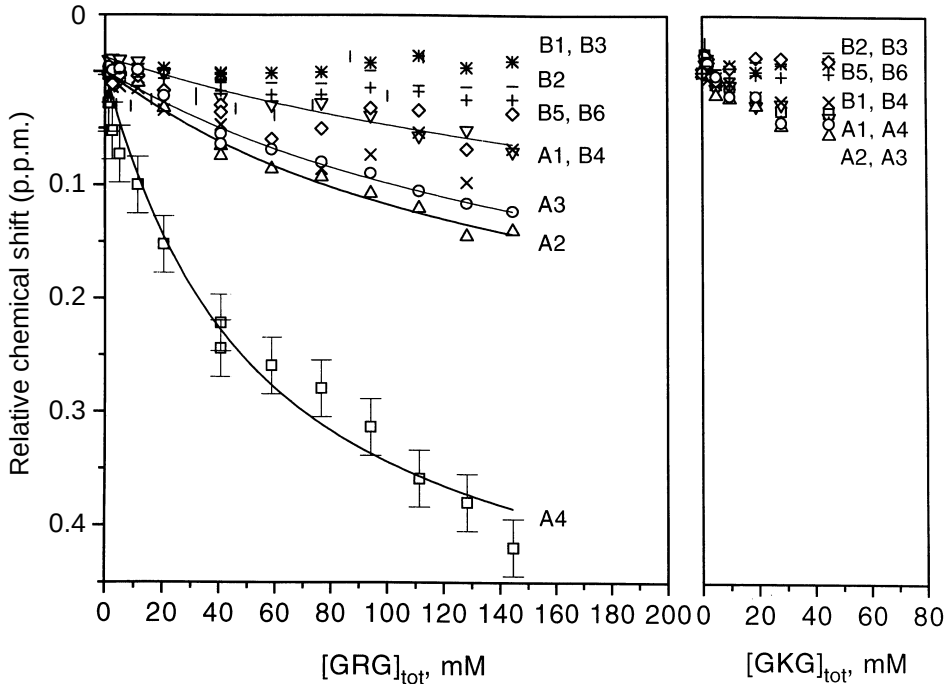

Figure 3 ^{13}C shift changes in disaccharide with peptide concentration

Relative ^{13}C chemical shifts for each protonated carbon resonance are plotted against the concentration of GRG (left panel) and GKG (right panel). Carbon positions in the A and B rings are indicated next to the data points. Some curves were fitted as described in the text. Solution conditions are pH 6.0, no added salt, at 278 K.

negatively charged by greater than 95%. All studies discussed below have therefore been done at pH values greater than pH 4.5.

Addition of increasing concentrations of N- and C-terminally blocked GRG and GKG produces heparin disaccharide chemical shift changes indicated in Figures 3 (left panel) and 3 (right panel) respectively. GRG produces the greater chemical shift changes, with the uronate carbon A4 being shifted the most (by 0.45 p.p.m.), followed by A2, A3 and A1. The glucosamine ring carbons are least shifted. For GKG (Figure 3, right panel), carbons A2, A3, B1, A4 and B4 are likewise shifted the most. In this case, however, A4 is clearly not the most highly shifted. These data indicate that the guanidino group of arginine is more effective at interacting with the heparin disaccharide than is the amine group of lysine. Moreover, in each case, uronate residue carbons are more highly shifted, indicating stronger peptide interactions at this heparin disaccharide residue.

Because the disaccharide A4 chemical shift changes are greater with GRG titration (Figure 3, left panel), these data were fitted assuming a 1:1 binding of GRG to the disaccharide (solid line in Figure 3, left panel), which yielded an equilibrium dissociation binding constant of 30 mM. The theoretical curve, however, appears not to fit all data points equally well, suggesting that greater than 1:1 binding could be occurring. Furthermore, the observation that A ring ^{13}C resonances are more shifted than those in the B ring indicates that GRG interacts preferentially with the A ring, and smaller chemical shift changes with GKG relative to GRG indicate weaker overall binding of GKG to the disaccharide.

Performing the same pH titration series as shown in Figure 2 for pure heparin disaccharide (△) in the presence of a 4-fold excess of GRG shifts the titration curve (Figure 2, □). At higher pH values, the ^{13}C signal arising from A4 is shifted downfield. As the pH is lowered, the A4 ^{13}C chemical shifts are identical in the presence or absence of GRG. Fitting these titration data with the Henderson–Hasselbalch equation (dotted line) yields a pK_a value of 3.09 ± 0.01. This pK_a depression of 0.06 pH units is significant given the number of data points (12) fitted in each titration curve and the observation that at lower pH values disaccharide carbon chemical shifts in the presence and absence of GRG are the same. This pK_a shift suggests that the arginine guanidino group interacts directly with the uronic acid carboxylate group.

^{13}C spin–lattice T_1 relaxation rates for methyne and methylene carbons have been measured by the inversion recovery method. Relaxation curves were linear with regression coefficients greater than 0.98 (results not shown). Figure 4A shows ^{13}C T_1 values (two ^{13}C frequencies) for the disaccharide in the absence and presence of GRG at various peptide-to-heparin ratios, i.e. 1:1, 2:1 and 4:1. For the free disaccharide, the small variability in T_1 values among methyne carbons indicates that the disaccharide ring system is fairly 'rigid'. A4 and B6 relaxation is more rapid owing to carbon–carbon double-bond p electrons and the presence of two methylene protons respectively. Addition of increasing concentrations of GRG increases disaccharide carbon relaxation rates consistent with peptide–heparin interactions. Figure 4B gives ^{13}C T_1 values for GRG carbons in the absence and presence of heparin disaccharide at the same peptide-to-heparin ratios. Although these GRG carbon relaxation rates are increased in the presence of disaccharide, overall changes are small and often are within experimental error. For the arginine ^{13}Cδ, however, the effect is significant and supports the idea of direct interaction of the positively charged arginine guanidino group with the negatively charged heparin disaccharide.

Because GKG produced smaller disaccharide chemical shifts, it was expected that GKG in the presence of heparin also would produce smaller T_1 effects. Figure 5 shows disaccharide ^{13}C T_1

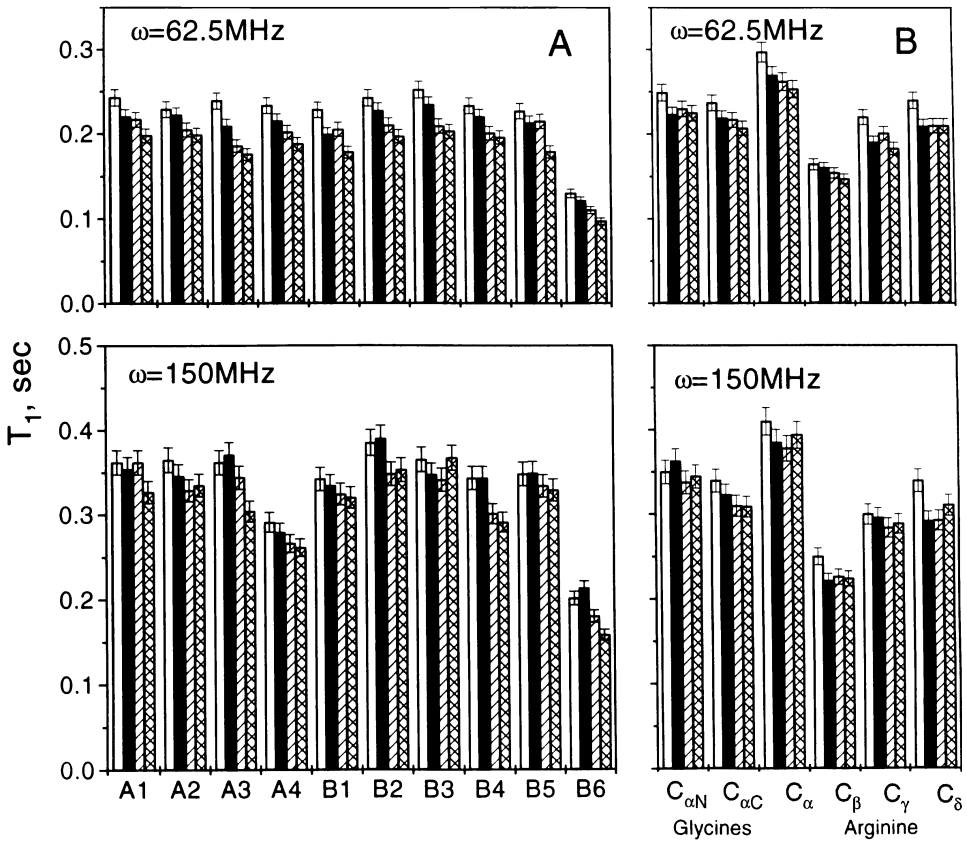

Figure 4 ^{13}C T_1 values for heparin disaccharide and GRG

(**A**) ^{13}C T_1 values for heparin disaccharide in the presence and absence of increasing concentrations of GRG are shown for two ^{13}C NMR frequencies, 62.5 and 150 MHz. For each A and B ring carbon position a tetrad of bars from left to right gives relaxation parameters for pure disaccharide and disaccharide-to-GRG molar ratios of 1:1, 1:2 and 1:4. (**B**) ^{13}C T_1 values for GRG in the presence and absence of increasing concentrations of heparin disaccharide are shown for two ^{13}C NMR frequencies, 62.5 and 150 MHz. For each GRG carbon position a tetrad of bars from left to right gives relaxation parameters for pure GRG and disaccharide-to-GRG molar ratios of 1:1, 1:2 and 1:4.

values for pure heparin and for heparin in the presence of an 8-fold molar excess of GKG and GRG. The 8:1 peptide-to-heparin ratio for GRG supplements data shown in Figure 4A, which go up to a ratio of 4:1. This gives a better comparison with maximal GKG effect. Even at the 8:1 ratio, T_1 values are only significantly affected for A3, A4 and B1 carbons. All GKG effects are less than with GRG, consistent with chemical shift changes noted above.

For a disaccharide-to-GRG ratio of 1:4, the effect of salt (NaCl) on ^{13}C T_1 relaxation was investigated (results not shown). NaCl concentrations of 1, 3, 10, 30, 100 and 300 mM were used. Minimal effects were found at salt concentrations below about 100 mM. In general, ^{13}C T_1 values are increased in the presence of NaCl, indicating weaker interactions between the heparin disaccharide and GRG. This is consistent with the idea that electrostatic forces modulate these peptide–heparin interactions.

Diffusion tensor calculations

Diffusion tensor calculations are simplified if molecular internal motions need not be considered, i.e. if one assumes an internally 'rigid' molecule. Because the glucosamine B ring exists in the chair form in solution, the primary concern about intra-ring bond rotations is for an equilibrium that is known to occur in solution between two half-chair forms of the uronate ring A ($^2H_1$–$^1H_2$) [41]. $^3J_{ik}$ coupling constants derived from a high-resolution double-quantum-filtered COSY experiment ($J_{1,2}$ 5.3 Hz, $J_{2,3}$ 4.8 Hz and $J_{3,4}$ 4.7 Hz) are consistent with those given by Ragazzi et al. [41] to support the presence of an equilibrium between only these two conformers. Because the $^2H_1$ population is about 10% populated [41], it could contribute to observed relaxation effects. The influence of each conformer on the diffusion tensor, however, is addressed below by performing calculations for both $^2H_1$ and $^1H_2$ forms.

T_1 values and ^1H–^1H inter-residue NOEs indicate that glycosidic bond rotations are relatively constrained. T_1 values for all methyne carbons are nearly the same for both rings and yield motional order parameters [36,37] of 0.84 (A1), 0.86 (A2), 0.85 (A3), 0.95 (A4), 0.89 (B1), 0.82 (B2), 0.82 (B3), 0.88 (B4), 0.89 (B5) and 0.77 (B6). Most S^2 values range from 0.82 to 0.89. For the A1–B4 glycosidic bond, A1 and A4 order parameters indicate angular variations of about $\pm 30°$ [36,37] with corrections being made for recoil effects resulting from motions of one ring relative to the other [38]. When calibrated against the B2–B4 (or B3–B5) inter-proton NOE using a distance of 2.72 Å, the A1–B4 NOE gives an average distance constraint of 2.28 Å compared with 2.39 Å from our calculated structure or to 2.36 Å from the Ragazzi et al. [41] structure. This NOE-derived distance indicates the presence of a relatively well defined conformational population, consistent with high motional order parameters discussed above. For $^2H_1$ and $^1H_2$ uronate conformations, the A1–B4 distance is nearly equal.

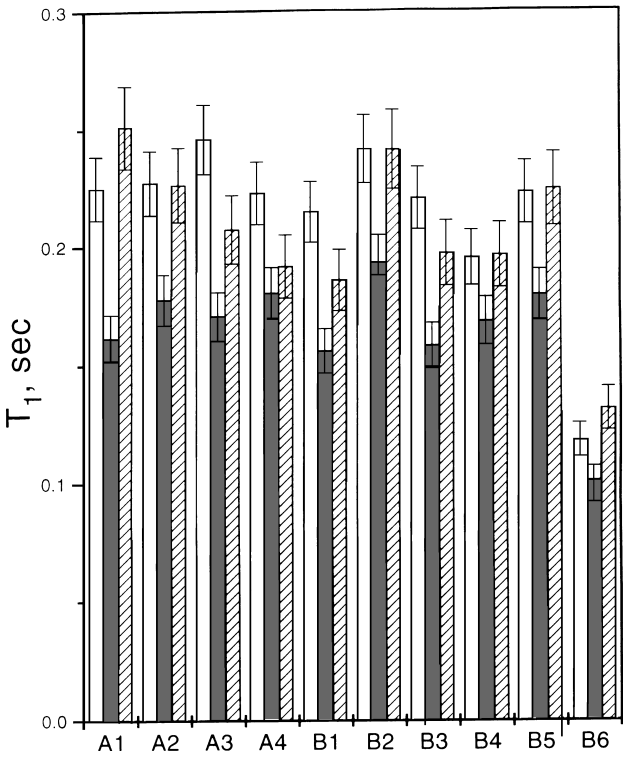

Figure 5 ^{13}C T_1 values for disaccharide with and without GKG

^{13}C (62.5 MHz) T_1 values for heparin disaccharide in the presence and absence of 8-fold molar excess of GRG and GKG are shown. For each A and B ring carbon position a triad of bars from left to right gives relaxation parameters for pure disaccharide, disaccharide with GRG, and disaccharide with GKG.

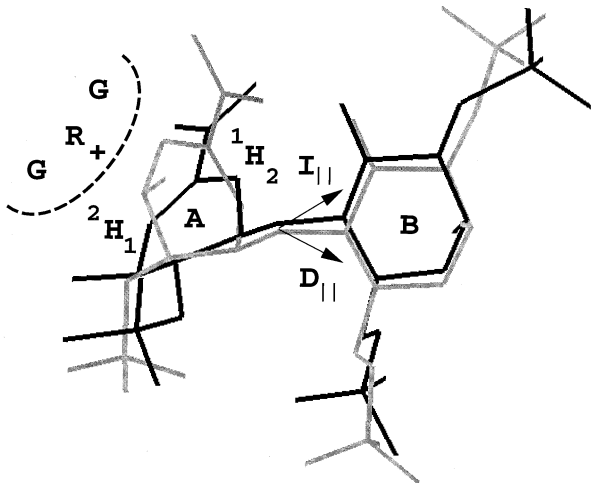

Figure 6 Average disaccharide conformation indicating $I_{\parallel}$ and $D_{\parallel}$

Two heparin disaccharide conformations are shown for $^2H_1$ (black) and $^1H_2$ (grey) forms of the uronic acid ring A. $I_{\parallel}$ for either conformation nearly bisects the A and B rings as indicated. The preferential orientation for GRG interacting with the disaccharide is shown.

Ten CH motional vectors are available for diffusion tensor analysis: four CHs in the A ring and five CHs and one CH_2 (average) in the B ring. Depending on ring geometry, certain of these vectors will be collinear or nearly collinear and therefore redundant. T_1 values therefore give six differently oriented CH motional vectors (three within each ring) that can be used to derive diffusion model parameters: perpendicular and parallel components of the diffusion tensor, $D_{\perp}$ and $D_{\parallel}$ respectively, and the orientation of the diffusion tensor symmetry axis in the molecular frame. The correctness of intra-ring conformations $^1H_2$ or $^2H_1$ for the uronate residue A and chair for the glucosamine residue was tested by using different sets of assumed collinear CH motional vectors. Because trends in the diffusion coefficients (discussed below) are the same, the assumption is supported. The molecular frame is defined by the components of the moment of inertia tensor calculated by using a 'rigid' structure for the disaccharide. The minimum energy structure calculated for the disaccharide (see the Materials and methods section) is shown in Figure 6 for both uronic acid ring A half-chair forms. Since parallel ($I_{\parallel}$) and perpendicular ($I_{\perp}$) components to the moment of inertia tensor yield $I_{\parallel}/I_{\perp}$ of about 0.5, a symmetric top motional model was used to calculate diffusion tensor components. To sample the most probable range of conformational space accessible to the disaccharide from internal rotations, the glycosidic bond angle was varied in moment of inertia and diffusion tensor calculations. A series of 'rigid' disaccharide conformations was generated by fixing the individual ring conformations ($^2H_1$ or $^1H_2$ for A and chair for B) and varying the glycosidic bond angles within the angular deviations defined by motional order parameters, i.e. $\pm 30°$ from the average calculated structure (the actual angles used were $\pm 6°$, 12°, 18°, 24° and 30°).

$D_{\perp}$, $D_{\parallel}$ and the angle α between $I_{\parallel}$ and $D_{\parallel}$ were calculated as a function of the disaccharide-to-GRG ratio. Results for the starting structure and the simple average over all structures ($\pm$S.D.) for each uronate half-chair form are given in Table 1. Large deviations of $D_{\parallel}$ from the $I_{\parallel}$ axis (Figure 6) are most probably due to strong electrostatic interactions of the disaccharide with the solvent, which was omitted for the *in vacuo* moment of inertia tensor calculations. For all conformations, $D_{\parallel}$ is greater than $D_{\perp}$, indicating that differences in half-chair forms do not greatly influence the average diffusion tensor. On addition of GRG, $D_{\perp}/D_{\parallel}$ is decreased, indicating that GRG is oriented along the $D_{\parallel}$ axis of the disaccharide as depicted in Figure 6. Because chemical shift changes are greatest at the uronate residue and at arginine Cδ carbon, Figure 6 shows the arginine residue (GR^+G) interacting with the A ring.

DISCUSSION

Heparin and similar polysulphated GAG binding to proteins is modulated by electrostatic interactions. Peptide sequences that have been identified as heparin-binding domains usually involve clusters of basic amino acids [17,19–22]. Interactions between proteins and heparin/heparin-like GAGs can be specific or non-specific. Platelet factor 4 [44] and thrombin [45] exemplify electrostatically modulated, non-specific heparin binding, whereas basic FGF-2 and hepatocyte growth factor [13] recognize specific groups on heparin. FGF-2 interacts specifically with GlcN *N*-sulphate and IdoA 2-*O*-sulphate groups [8,46,47]; however, a single IdoA 2-*O*-sulphate group in a defined pentasaccharide sequence is crucial [8] and the GlcN 6-*O*-sulphates are redundant, neither contributing to nor interfering with FGF-2 binding [8,46,47]. In contrast, binding of hepatocyte growth factor to heparin/heparan sulphate seems to depend primarily on GlcN 6-*O*-sulphates [13]. These findings suggest that different proteins might bind to heparin/heparan sulphate in a differential and specific manner.

In the present study it has been shown that GRG preferentially interacts at the uronate residue of the heparin disaccharide as

Table 1 Diffusion tensor calculations

Abbreviation used: Dis, disaccharide.

	Starting structure						Average			
	$10^8 \times D_{\parallel}$ (s^{-1})		$D_{\perp}/D_{\parallel}$		α		$D_{\parallel}$		$D_{\perp}/D_{\parallel}$	
[Dis]:[GRG]	$^2H_1$	$^1H_2$	$^2H_1$	$^1H_2$	$^2H_1$	$^1H_2$	$^2H_1$	$^1H_2$	$^2H_1$	$^1H_2$
1:0	11.8	10.1	0.47	0.64	61	79	12.8 ± 1.6*	9.9 ± 0.6*	0.42 ± 0.1*	0.67 ± 0.07*
1:1	13.7	9.5	0.26	0.62	60	81	13.1 ± 0.9	10.4 ± 1.6	0.31 ± 0.05*	0.54 ± 0.14*
1:2	12.7	10.1	0.26	0.44	73	69	12.0 ± 0.7	9.1 ± 0.8	0.32 ± 0.04*	0.55 ± 0.09*
1:4	11.1	7.2	0.25	0.71	68	62	10.1 ± 0.8	7.6 ± 0.4	0.35 ± 0.07*	0.65 ± 0.07*

* Standard deviation from the average value.

opposed to the more sulphated glucosamino residue. ^{13}C chemical shift and spin–lattice (T_1) relaxation rate changes and diffusion tensor analysis, as well as a carboxylate group pK_a depression, support a model where the arginine guanidino group is oriented between the uronate residue carboxylate and 2-*O*-sulphate groups. It should be emphasized that the disaccharide used here contains an unsaturated uronate residue rather than the authentic iduronate. The presence of a double bond between carbons A4 and A5 makes for a more planar ring system and, for example, increases the distance between sulphate and carboxylate groups. At this point it is unknown how this modification will affect GRG or GKG binding to a true heparin disaccharide unit. Indirectly, however, the observation that GRG interacts more strongly than GKG with the uronate-containing disaccharide supports the idea that we are selecting for at least some of the salient properties that dictate peptide binding to larger heparin species. The arginine guanidino group has been identified by others to promote stronger interactions with heparin than does the lysine amine group.

By examining the frequency of amino acids in proteins in sites known to bind heparin in addition to combinatorial peptides with high affinity for heparin and heparan sulphate agarose, Caldwell et al. [48] observed a preference for arginine over lysine, with histidine falling a distant third in modulating GAG binding. Gelman and co-workers [49–51] demonstrated that polyarginine α-helix denatured at a higher temperature when binding to GAGs than an analogous polylysine polymer [49]. Fromm et al. [52] discovered that even blocked arginines bind more tightly to heparin than does blocked lysine, suggesting that hydrogen bonding of the arginine guanidino group to heparin plays a role in the binding process. Arginines may have a structural feature in their basic side chain that enhances binding. Mascotti and Lohman [53] also concluded that arginines most probably participate in more extensive hydrogen bonding interactions with heparin. In this context, it is interesting to note that arginines are essential for the binding of thrombin and antithrombin-III to heparin [54,55].

In structurally homologous phosphoryl–cation interactions, arginine also plays a more important role than lysine or histidine. Conserved protein domains that bind phosphotyrosine (SH2 domains) contain more arginine than lysine residues [56,57] presumably owing to the avid interaction of arginine with phosphoryl anions, compared with the interaction of lysine with the phosphoryl anion. From X-ray crystallographic and computer modelling studies [52,58], it is apparent that guanidino groups can form fewer, albeit stronger, hydrogen bonds with sulphates/phosphates than do ammonium cations. The guanidinium cation rather than the ammonium cation may form an inherently stronger electrostatic interaction with the sulphate anion. In the context of Pearson's concept of soft acid, soft base interactions [59], arginine, a large diffuse cation (soft), is ideally suited to interact with large (soft) bioanions, such as sulphate and phosphate. Riordan et al. [60] suggest that in the natural environment arginyl residues play a unique role in anion recognition. It has even been suggested that arginine appeared later in evolution to perform important biological functions [60–62].

From analysis of heparin–tripeptide equilibrium binding isotherms, Mascotti and Lohman [53] found that the tripeptides KWK and RWR bound heparin with association binding constants of 7.0 mM^{-1} and 13 mM^{-1}, respectively. RWR bound heparin about 2-fold more strongly than did KWK. Mascotti and Lohman [53] suggested, however, that these short peptides bind heparin in a non-specific electrostatic fashion, with the prime factor determining stability being the charge density of the linear polyelectrolyte. For the GRG–heparin disaccharide system, preferential interactions are observed. Mascotti and Lohman [53], however, used high-molecular-mass heparin (16 kDa cut off) and double R- or double K-containing tripeptides with charged termini. Both the size differential between the peptides and the heparin as well as the charge distribution of the tripeptide might be more favourable to non-specific interactions. These GRG and GKG studies used a well-defined heparin fraction and tripeptides with blocked N- and C-termini. Alternatively, the presence of the uronate C-4–C-5 double bond may contribute to this observation. This is currently under investigation by using larger, homogeneous heparin fractions.

This work was supported by grants from the National Institutes of Health (GM38060) and the National Science Foundation (MCB-9420203) and benefited from the use of the high-field NMR facility at the University of Minnesota.

REFERENCES

1 Jeanloz, R. W. (1975) Adv. Exp. Med. Biol. **52**, 3–12
2 Lindahl, U. (1974) Int. Rev. Sci., Org. Chem. Ser. **2**, 283–289
3 Perlin, A. S., Mackie, D. M. and Dietrich, C. P. (1971) Carbohydr. Res. **18**, 185–192
4 Kjellen, L. and Lindahl, U. (1991) Annu. Rev. Biochem. **60**, 443–475
5 Lindahl, U., Lidholt, K., Spillmann, D. and Kjellen, L. (1994) Thromb Res. **75**, 1–32
6 Spillmann, D. and Lindahl, U. (1994) Curr. Opin. Struct. Biol. **4**, 677–682
7 Tyrrell, D. J., Ishihara, M., Rao, N., Horne, A., Kiefer, M. C., Stauber, G. B., Lam, L. H. and Stack, R. J. (1993) J. Biol. Chem. **268**, 4684–4689
8 Maccarana, M., Casu, B. and Lindahl, U. (1993) J. Biol. Chem. **268**, 23898–23905
9 Tanaka, Y., Adams, D. H., Hubscher, S., Hirano, H., Siebenlist, U. and Shaw, S. (1993) Nature (London) **361**, 79–82
10 Webb, L. M., Ehrengruber, M. U., Clark-Lewis, I., Baggiolini, M. and Rot, A. (1993) Proc. Natl. Acad. Sci. U.S.A. **90**, 7158–7162
11 Witt, D. P. and Lander, A. D. (1994) Curr. Biol. **4**, 394–400

12 Tessler, S., Rockwell, P., Hicklin, D., Cohen, T., Levi, B. Z., Witte, L., Lemischka, I. R. and Neufeld, G. (1994) J. Biol. Chem. **269**, 12456–12461
13 Lyon, M., Deakin, J. A., Mizuno, K., Nakamura, T. and Gallagher, J. T. (1994) J. Biol. Chem. **269**, 1216–1223
14 Thompson, L. D., Pantoliano, M. W. and Springer, B. A. (1994) Biochemistry **33**, 3831–3840
15 Thompson, S. A., Higashiyama, S., Wood, K., Pollitt, N. S., Damm, D., McEnroe, G., Garrick, B., Ashton, N., Lau, K. and Hancock, N. (1994) J. Biol. Chem. **269**, 2541–2549
16 Norgard-Sumnicht, K. E., Varki, N. M. and Varki, A. (1993) Science **261**, 480–483
17 DeLisser, H. M., Yan, H. C., Newman, P. J., Muller, W. A., Buck, C. A. and Albelda, S. M. (1993) J. Biol. Chem. **268**, 16037–16046
18 Raulo, E., Chernousov, M. A., Carey, D. J., Nolo, R. and Rauvala, H. (1994) J. Biol. Chem. **269**, 12999–13004
19 Cardin, A. D. and Weintraub, H. J. R. (1989) Arteriosclerosis **9**, 21–32
20 Sobel, M., Soler, D. F., Kermode, J. C. and Harris, R. B. (1992) J. Biol. Chem. **267**, 8857–8862
21 Drake, S. L., Varnum, J., Mayo, K. H., Letourneau, P. C., Furcht, L. T. and McCarthy, J. B. (1993) J. Biol. Chem. **268**, 15859–15867
22 Murphy-Ulrich, J. E., Gurusiddappa, S., Frazier, W. A. and Hook, M. (1993) J. Biol. Chem. **268**, 26784–26789
23 Mourey, L., Samama, J. P., Delarue, M., Pepitou, M., Choay, J. and Moras, D. (1993) J. Mol. Biol. **232**, 223–241
24 van Tilbeurgh, H., Roussel, A., Lalouel, J. M. and Cambillau, C. (1994) J. Biol. Chem. **269**, 4626–4633
25 Eriksson, A. E., Cousens, L. S. and Matthews, B. W. (1993) Protein Sci. **2**, 1274–1284
26 Mayo, K. H., Ilyina, E., Roongta, V., Dundas, M., Joseph, J., Lai, C. K., Maione, T. and Daly, T. J. (1995) Biochem. J. **312**, 357–365
27 Linhardt, R. J., Rice, K. G., Kim, Y. S., Lohse, D. L., Wang, H. M. and Loganathan, D. (1988) Biochem. J. **254**, 781–787
28 Loganathan, D., Wang, H. M., Mallis, L. M. and Linhardt, R. J. (1990) Biochemistry **29**, 4362–4368
29 Stewart, J. M. and Young, J. D. (1984) Solid Phase Peptide Synthesis, 2nd edn., Pierce Chemical Co., Rockford, IL
30 Merchant, Z. M., Kim, Y. S., Rice, K. G. and Linhardt, R. J. (1985) Biochem. J. **229**, 369–377
31 Piantini, U., Srensen, O. W. and Ernst, R. R. (1982) J. Am. Chem. Soc. **104**, 6800–6805
32 Shaka, A. J. and Freeman, R. (1983) J. Magn. Reson. **51**, 161–169
33 Wüthrich, K. (1986) NMR of Proteins and Nucleic Acids, Wiley-Interscience, New York
34 States, D. J., Haberkorn, R. A. and Ruben, D. J. (1982) J. Magn. Reson. **48**, 286–293
35 Daragan, V. A. and Mayo, K. H. (1993) Biochemistry **32**, 11488–11499
36 Lipari, G. and Szabo, A. (1982) J. Am. Chem. Soc. **104**, 4546–4559
37 Lipari, G. and Szabo, A. (1982) J. Am. Chem. Soc. **104**, 4559–4570
38 Daragan, V. A. and Mayo, K. H. (1994) J. Phys. Chem. **98**, 10949–10956
39 Werbelow, L. G. and Grant, D. M. (1977) Adv. Magn. Reson. **9**, 189–299
40 Mulloy, B., Forster, M. J., Jones, C. and Davies, D. B. (1993) Biochem. J. **293**, 849–857
41 Ragazzi, M., Ferro, D. R., Provasoli, A., Pumilia, P., Cassinari, A., Torri, G., Guerrini, M., Casu, B., Nader, H. B. and Dietrich, C. P. (1993) J. Carbohydrate Chem. **12**, 523–535
42 Wang, H.-M., Loganathan, D. and Linhardt, R. J. (1991) Biochem. J. **278**, 689–695
43 Casu, B. and Gennard, U. (1975) Carbohydr. Res. **39**, 168–176
44 Stuckey, J. A., St. Charles, R. and Edwards, B. F. P. (1992) Proteins Struct. Funct. Genet. **14**, 277–287
45 Olson, S. T. and Bjork, I. (1991) J. Biol. Chem. **266**, 6353–6364
46 Habuchi, H., Suzuki, S., Saito, T., Tamura, T., Harada, T., Yoshida, K. and Kimata, K. (1992) Biochem. J. **285**, 805–813
47 Turnbull, J. E., Fernig, D. G., Ke, Y., Wilkinson, M. C. and Gallagher, J. T. (1992) J. Biol. Chem. **267**, 10337–10341
48 Caldwell, E. E. O., Nadkarni, V. D., Fromm, J. R., Linhardt, R. J. and Weiler, J. M. (1995) Int. J. Biochem. Cell Biol., in the press
49 Gelman, R. A. and Blackwell, J. (1974) Biopolymers **13**, 139–156
50 Gelman, R. A., Glasner, D. N. and Blackwell, J. (1973) Biopolymers **12**, 1223–1232
51 Gelman, R. A., Rippon, W. B. and Blackwell, J. (1973) Biopolymers **12**, 541–558
52 Fromm, J. R., Hileman, R. E., Caldwell, E. E. O., Weiler, J. M. and Linhardt, R. J. (1995) Arch. Biochem. Biophys. **323**, 279–287
53 Mascotti, D. P. and Lohman, T. M. (1995) Biochemistry **34**, 2908–2915
54 Pomerantz, M. W. and Owen, W. G. (1978) Biochim. Biophys. Acta **535**, 66–77
55 Machovich, R., Staub, M. and Patthy, L. (1978) Eur. J. Biochem. **83**, 473–477
56 Koch, C. A., Anderson, D., Moran, M. F., Ellis, C. and Pawson, T. (1991) Science **252**, 668–674
57 Waksman, G., Shoelson, S. E., Pant, N., Cowburn, D. and Kuriyan, J. (1993) Cell **72**, 779–790
58 Cotton, F. A., Hazen, E. E., Day, V. W., Larsen, S., Norman, J. G., Wong, S. T. K. and Johnson, K. H. (1973) J. Am. Chem. Soc. **95**, 2367–2369
59 Pearson, R. G. (1963) J. Am. Chem. Soc. **85**, 3533–3539
60 Riordan, J. F., McElvany, K. D. and Borders, C. L., Jr. (1977) Science **195**, 884–886
61 Wallis, M. (1974) Biochem. Biophys. Res. Commun. **56**, 711–716
62 Jukes, T. H. (1973) Biochem. Biophys. Res. Commun. **53**, 709–714

Received 9 October 1995/10 November 1995; accepted 6 December 1995